axioms

MDPI

Article

Fractal Fractional Derivative Models for Simulating Chemical Degradation in a Bioreactor

Ali Akgül [1,2,3] and J. Alberto Conejero [4,*]

[1] Department of Mathematics, Art and Science Faculty, Siirt University, 56100 Siirt, Turkey; aliakgul00727@gmail.com
[2] Department of Computer Science and Mathematics, Lebanese American University, Beirut P.O. Box 13-5053, Lebanon
[3] Department of Mathematics, Mathematics Research Center, Near East University, Near East Boulevard, 99138 Mersin, Turkey
[4] Instituto Universitario de Matemática Pura y Aplicada, Universitat Politècnica de València, 46022 València, Spain
* Correspondence: aconejero@upv.es

Abstract: A three-differential-equation mathematical model is presented for the degradation of phenol and p-cresol combination in a bioreactor that is continually agitated. The stability analysis of the model's equilibrium points, as established by the study, is covered. Additionally, we used three alternative kernels to analyze the model with the fractal–fractional derivatives, and we looked into the effects of the fractal size and fractional order. We have developed highly efficient numerical techniques for the concentration of biomass, phenol, and p-cresol. Lastly, numerical simulations are used to illustrate the accuracy of the suggested method.

Keywords: bioreactor model; numerical methods; fractal–fractional derivatives; numerical simulations

MSC: 26A33, 34A08, 35R11.

Citation: Akgül, A.; Conejero, J.A. Fractal Fractional Derivative Models for Simulating Chemical Degradation in a Bioreactor. *Axioms* **2024**, *13*, 151. https://doi.org/10.3390/axioms13030151

Academic Editors: Nohe R. Cazarez-Castro, Selene L. Cardenas-Maciel, Jorge A. Lopez-Renteria

Received: 18 December 2023
Revised: 11 February 2024
Accepted: 20 February 2024
Published: 26 February 2024

1. Introduction

In a bioreactor, chemical degradation is the process by which certain chemicals or compounds are broken down or changed by living things in the bioreactor's controlled environment. Bioreactors are widely used to support biological processes, including fermentation, enzyme manufacturing, and wastewater treatment in various industries, including pharmaceuticals, biotechnology, wastewater treatment, and food production.

Many scientific papers have presented the isolation and work of microbial species with higher-degradation action and abilities to degrade chemical compounds [1]. Many isolated bacteria have been investigated in [2]. The biodegradation of one or all chemical parts hinges on the composition of the specific mixture and the utilized microorganisms [3–6]. Fractional calculus is an influential extension of the classical derivatives. Fractional differential equations (FDEs) have recently been implemented in different fields. Many authors have worked on these equations, such as the KdV equation [7], advection-dispersion equation [8], telegraph equation [9], Schrodinger equation [10], heat equation [11], convection-diffusion equation [12], Fokker Planck equation [13], and Lambert–Beer equation [14,15]. Some of the FDEs do not have exact solutions. Therefore, it is required to work on numerical methods to solve the mentioned equations, such as solving nonlinear fractional diffusion wave equations with the homotopy analysis technique [16], solving PDEs of fractal order by Adomian decomposition method [17]. In [1], the authors have given a bioreactor model but do not consider the bacteria's death rate and general configuration of the reactor. We have provided the bioreactor model with the fractal–fractional operators. The model with fractal–fractional derivatives has never been analyzed so far. Our model includes the death

rate of bacteria, which is important in the process's environment. We also consider the general configuration of the reactor, where our model includes a membrane and continuous reactor. Additionally, we fractionalize the model and apply a novel numerical technique to achieve the numerical simulations. In these simulations, we use different fractal dimensions and fractional orders. For more details, see [18–30].

We organize our manuscript as follows. Problem formulation is performed in Section 2. In Section 3, we discuss the model's analysis in the classical case and present the equilibrium and stability analysis. Next, we explore the analysis of the model with three different kernels viz. the power-law kernel (Section 4), the exponential-decay kernel (Section 5), and the Mittag–Leffler function (Section 6). Finally, in Section 7, we illustrate the numerical simulations of the proposed models.

2. Preliminaries

The following definitions of fractional differentiation operator and fractal–fractional integral operator with three different kernels are taken from [21] .

Definition 1. *The fractional differentiation operator with the power-law-type kernel is described as:*

$$ {}^{FFP}_{c}D^{\alpha,\eta}_{t} f(t) = \frac{1}{1-\alpha}\frac{d}{du^{\eta}}\int_{c}^{t} f(s)(t-s)^{-\alpha}ds,\ 0<\alpha,\eta\leq 1, \tag{1} $$

where,

$$ \frac{df(s)}{ds^{\eta}} = \lim_{t\to s}\frac{f(t)-f(s)}{t^{\eta}-s^{\eta}} \tag{2} $$

Definition 2. *The fractional differentiation operator with the exponential-decay-type kernel is described as:*

$$ {}^{FFE}_{c}D^{\alpha,\eta}_{t} f(t) = \frac{M_1(\alpha)}{1-\alpha}\frac{d}{dt^{\eta}}\int_{c}^{t} f(s)\exp\Big(\frac{-\alpha}{1-\alpha}(t-s)\Big)ds,\ 0<\alpha,\eta\leq 1. \tag{3} $$

Definition 3. *The fractional differentiation operator with the Mittag–Leffler-type kernel is described as:*

$$ {}^{FFM}_{c}D^{\alpha,\eta}_{t} f(t) = \frac{AB(\alpha)}{1-\alpha}\frac{d}{dt^{\eta}}\int_{c}^{t} f(s)E_{\alpha}\Big(\frac{-\alpha}{1-\alpha}(t-s)^{\alpha}\Big)ds,\ 0<\alpha,\eta\leq 1, \tag{4} $$

where $AB(\alpha) = 1-\alpha+\frac{\alpha}{\Gamma(\alpha)}$.

Definition 4. *The fractional integration operator with the power-law-type kernel is described as:*

$$ {}^{FFP}_{0}I^{\alpha,\eta}_{t} f(t) = \frac{\eta}{\Gamma(\alpha)}\int_{0}^{t}(t-s)^{\alpha-1}s^{\tau-1}\phi(s)ds. \tag{5} $$

Definition 5. *The fractional integration operator with the exponential-decay-type kernel is described as:*

$$ {}^{FFE}_{0}I^{\alpha,\eta}_{t} f(t) = \frac{\alpha\eta}{M_1(\alpha)}\int_{0}^{t} s^{\alpha-1}f(s)ds + \frac{\tau(1-\alpha)t^{\tau-1}}{M_1(\alpha)}\phi(t). \tag{6} $$

Definition 6. *The fractional integration operator with the Mittag–Leffler-type kernel is described as:*

$$ {}^{FFM}_{0}I^{\alpha,\eta}_{t} f(t) = \frac{\alpha\eta}{AB(\alpha)}\int_{0}^{t} s^{\alpha-1}f(s)(t-s)^{\alpha-1}ds + \frac{\tau(1-\alpha)t^{\tau-1}}{AB(\alpha)}f(t). \tag{7} $$

Here, we present the model to be investigated in this research. We present the model as:

$$\frac{dS_{ph}}{dt} = D\left(S_{ph0} - S_{ph}\right) - k_{ph} \cdot \mu\left(S_{ph}, S_{cr}\right) \cdot X, \tag{8}$$

$$\frac{dS_{cr}}{dt} = D(S_{cr0} - S_{cr}) - k_{cr} \cdot \mu\left(S_{ph}, S_{cr}\right) \cdot X, \tag{9}$$

$$\frac{dX}{dt} = -D\beta X + \mu\left(S_{ph}, S_{cr}\right)X, \tag{10}$$

$$\mu\left(S_{ph}, S_{cr}\right) = \frac{\mu_{max(ph)}S_{ph}}{K_{s(ph)} + S_{ph} + \frac{S_{ph}^2}{k_{i(ph)}} + I_{cr/ph}S_{cr}} + \frac{\mu_{max(cr)}S_{cr}}{K_{s(cr)} + S_{cr} + \frac{S_{cr}^2}{k_{i(cr)}} + I_{ph/cr}S_{ph}}, \tag{11}$$

The model parameters and variables are detailed in [1]. The parameter β is presented in the general configuration. When $\beta = 1$, we have continued the reactor. When $\beta = 0$, we have a membrane reactor.

3. Analysis of the Model in Classical Sense

Now, we begin with analyzing the properties of the model in classical sense.

We consider the number of equilibrium solutions of the model ((8)–(10)). It is obvious that the model has a branch of the washout given by

$$E_0 = (S_{ph}, S_{cr}, X) = \left(S_{ph0}, S_{cr0}, 0\right). \tag{12}$$

We obtain the steady state solution of ((8)–(10)) by setting to zero the right side. From the model ((8)–(10)), we have:

$$\begin{aligned} S_{cr} &= \frac{S_{cr0}k_{ph} + k_{cr}(S_{ph} - S_{ph0})}{k_{ph}}, \\ X &= \frac{D\left(S_{ph0} - S_{ph}\right)}{k_{ph}\left(\beta D\right)}. \end{aligned} \tag{13}$$

$$f = \begin{pmatrix} -k_{cr}\mu(s_{ph},s_{cr})X \\ \mu(s_{ph},s_{cr})X \end{pmatrix} \quad \rightarrow \quad F = \begin{bmatrix} \frac{\partial\mu(s_{ph},s_{cr})(-k_{cr})X}{\partial(s_{ph},s_{cr})X} & -k_{cr}\mu(s_{ph},s_{cr}) \\ \\ \frac{\partial\mu(s_{ph},s_{cr})X}{\partial(s_{ph},s_{cr})X} & \mu(s_{ph},s_{cr})k_{cr}(s_{ph},s_{cr}) \end{bmatrix}$$

$$V = \begin{pmatrix} -D(s_{cr0}-s_{cr}) \\ D\beta X \end{pmatrix} \quad \rightarrow \quad V = \begin{bmatrix} D & 0 \\ \\ 0 & D\beta \end{bmatrix} \quad , V^{-1} = \begin{bmatrix} D\beta & 0 \\ \\ 0 & D \end{bmatrix}$$

$$FV^{-1} = \begin{bmatrix} 0 & -k_{cr}\mu(s_{ph},s_{cr}) \\ \\ 0 & \mu(s_{ph},s_{cr}) \end{bmatrix} \begin{bmatrix} D & 0 \\ \\ 0 & D\beta \end{bmatrix} = \begin{bmatrix} 0 & -\beta D k_{cr}\mu(s_{ph},s_{cr}) \\ \\ 0 & \beta D\mu(s_{ph},s_{cr}) \end{bmatrix}$$

$$det\left[\ FV^{-1} - \lambda I_2\ \right] = 0 \quad , \begin{vmatrix} -\lambda & -\beta D k_{cr}\mu(s_{ph},s_{cr}) \\ \\ 0 & \beta D\mu(s_{ph},s_{cr}) - \lambda \end{vmatrix} = 0$$

Thus, we obtain $\lambda_1 = 0, \quad \lambda_2 = \beta D\mu(s_{ph}, s_{cr}) = R_0$.

Lemma 1. *The steady state solution E_0 is locally asymptotically stable when $D > D_{cr}$ and is unstable when $D < D_{cr}$, where*

$$D_{cr} = \frac{k_{icr}k_{ph}(s_{cr0}k_{ph} - s_{ph0}k_{cr})^{-}max_{cr}}{\left[k_{icr}k_{ph}(K_{scr}k_{ph} + s_{cr0}k_{ph} - s_{ph0}k_{cr}) + (s_{cr}k_{ph} - s_{ph0}k_{cr})^2\right]\beta}.$$

Proof. We have

$$E_0 = (s_{ph}, s_{cr}, x) = (s_{ph0}, s_{cr0}, 0)$$

$$J(E_0) = \begin{bmatrix} -D - \frac{\partial \mu(s_{ph}, s_{cr})}{\partial s_{ph}} k_{ph} x & -\frac{\partial \mu(s_{ph}, s_{cr})}{\partial s_{ph}} k_{ph} x & -\mu(s_{ph}, s_{cr}) k_{ph} \\ -k_{cr} \frac{\partial \mu(s_{ph}, s_{cr})}{\partial s_{ph}} x & -D - \frac{\partial \mu(s_{ph}, s_{cr})}{\partial s_{ph}} k_{cr} x & -\mu(s_{ph}, s_{cr}) k_{cr} \\ \frac{\partial \mu(s_{ph}, s_{cr})}{\partial s_{ph}} x & -\frac{\partial \mu(s_{ph}, s_{cr})}{\partial s_{ph}} x & -D\beta + \mu(s_{ph}, s_{cr}) \end{bmatrix}$$

$$J(E_0) = \begin{bmatrix} -D & 0 & -\mu(s_{ph0}, s_{cr0}) k_{ph} \\ 0 & -D & -\mu(s_{ph0}, s_{cr0}) k_{cr} \\ 0 & 0 & -D\beta + \mu(s_{ph0}, s_{cr0}) \end{bmatrix}$$

where

$$\mu(s_{ph}, s_{cr}) = \frac{\mu_{max(ph)} s_{ph}}{K_{s(ph)} + s_{ph} + \frac{s_{ph}^2}{K_{i(ph)}} + I_{cr/ph} s_{cr}} + \frac{\mu_{max(cr)} s_{ph}}{K_{s(cr)} + s_{cr} + \frac{s_{cr}^2}{K_{i(cr)}} + I_{ph/cr} s_{ph}}$$

$$\det[J(E_0) - \lambda I_3] = \begin{vmatrix} -D - \lambda & 0 & -\mu(s_{ph}, s_{cr}) k_{ph} \\ 0 & -D - \lambda & -\mu(s_{ph}, s_{cr}) k_{cr} \\ 0 & 0 & \mu(s_{ph}, s_{cr}) - D\beta - \lambda \end{vmatrix} = 0$$

$$= (-D - \lambda)(-D - \lambda)(\mu(s_{ph}, s_{cr}) - D\beta - \lambda) = 0$$

$$\lambda_1 = -D, \quad \lambda_2 = -D, \quad \lambda_3 = -\beta D + \mu(s_{ph}, s_{cr})$$

and

$$\mu(s_{ph}, s_{cr}) = {}^{-} max_{ph} s_{ph0} (k_{sph} + s_{ph0} + \frac{s_{ph0}^2}{K_{i(ph)}} + I_{cr/ph} s_{cr0})^{-1}$$
$$+ {}^{-} max_{cr} s_{cr0} (k_{scr} + s_{cr0} + \frac{s_{cr0}^2}{K_{i(ph)}} + I_{ph/cr} s_{ph0})^{-1}$$
$$D_{cr} = \frac{k_{icr} k_{ph} (s_{cr0} k_{ph} - s_{ph0} k_{cr})^{-} max_{cr}}{\left[k_{icr} k_{ph} (K_{scr} k_{ph} + s_{cr0} k_{ph} - s_{ph0} k_{cr}) + (s_{cr} k_{ph} - s_{ph0} k_{cr})^2 \right] \beta}$$

If $D > D_{cr}$, then $\lambda_3 < 0$. Thus, all eigenvalues are negative. This shows that the steady state solution E_0 is locally asymptotically stable. □

4. Analysis of the Model with the Power-Law Kernel

Here, we analyze the model with fractional differentiation operator using the power-law kernel as:

$${}_0^{FFP} D_t^{\alpha,\eta} S_{ph} = D\Big(S_{ph0} - S_{ph}\Big) - k_{ph} \cdot \mu\Big(S_{ph}, S_{cr}\Big) \cdot X. \tag{14}$$

$${}_0^{FFP} D_t^{\alpha,\eta} S_{cr} = D(S_{cr0} - S_{cr}) - k_{cr} \cdot \mu\Big(S_{ph}, S_{cr}\Big) \cdot X. \tag{15}$$

$${}_0^{FFP} D_t^{\alpha,\eta} X = -D\beta X + \mu\Big(S_{ph}, S_{cr}\Big) X. \tag{16}$$

We have the following relation between the classical and fractal derivative [21]:

$$D^{\eta} f(t) = \frac{f'(t)}{\eta t^{\eta-1}}. \tag{17}$$

A relation between the classical derivative and the fractal derivative gives

$$ {}_0^{RL}D_t^{\alpha} S_{ph} = \eta t^{\eta-1}\Big(D\Big(S_{ph0} - S_{ph}\Big) - k_{ph} \cdot \mu\Big(S_{ph}, S_{cr}\Big) \cdot X\Big). \tag{18}$$

$$ {}_0^{RL}D_t^{\alpha} S_{cr} = \eta t^{\eta-1}\Big(D(S_{cr0} - S_{cr}) - k_{cr} \cdot \mu\Big(S_{ph}, S_{cr}\Big) \cdot X\Big). \tag{19}$$

$$ {}_0^{RL}D_t^{\alpha} X = \eta t^{\eta-1}\Big(-D\beta X + \mu\Big(S_{ph}, S_{cr}\Big)X\Big). \tag{20}$$

For simplicity, we define

$$A(t, S_{ph}, S_{cr}, X) = \eta t^{\eta-1}\Big(D\Big(S_{ph0} - S_{ph}\Big) - k_{ph} \cdot \mu\Big(S_{ph}, S_{cr}\Big) \cdot X\Big). \tag{21}$$

$$B(t, S_{ph}, S_{cr}, X) = \eta t^{\eta-1}\Big(D(S_{cr0} - S_{cr}) - k_{cr} \cdot \mu\Big(S_{ph}, S_{cr}\Big) \cdot X\Big). \tag{22}$$

$$C(t, S_{ph}, S_{cr}, X) = \eta t^{\eta-1}\Big(-D\beta X + \mu\Big(S_{ph}, S_{cr}\Big)X\Big). \tag{23}$$

Then, we obtain

$$ {}_0^{RL}D_t^{\alpha} S_{ph} = A(t, S_{ph}, S_{cr}, X). \tag{24}$$

$$ {}_0^{RL}D_t^{\alpha} S_{cr} = B(t, S_{ph}, S_{cr}, X). \tag{25}$$

$$ {}_0^{RL}D_t^{\alpha} X = C(t, S_{ph}, S_{cr}, X). \tag{26}$$

Applying the Riemann–Liouville integral yields:

$$S_{ph}(t) - S_{ph}(0) = \frac{1}{\Gamma(\alpha)} \int_0^t A(\tau, S_{ph}, S_{cr}, X)(t-\tau)^{\alpha-1} d\tau. \tag{27}$$

$$S_{cr}(t) - S_{cr}(0) = \frac{1}{\Gamma(\alpha)} \int_0^t B(\tau, S_{ph}, S_{cr}, X)(t-\tau)^{\alpha-1} d\tau. \tag{28}$$

$$X(t) - X(0) = \frac{1}{\Gamma(\alpha)} \int_0^t C(\tau, S_{ph}, S_{cr}, X)(t-\tau)^{\alpha-1} d\tau. \tag{29}$$

Discretizing the above equations at t_{n+1}, we receive:

$$S_{ph}(t_{n+1}) - S_{ph}(0) = \frac{1}{\Gamma(\alpha)} \int_0^{t_{n+1}} A(\tau, S_{ph}, S_{cr}, X)(t_{n+1}-\tau)^{\alpha-1} d\tau. \tag{30}$$

$$S_{cr}(t_{n+1}) - S_{cr}(0) = \frac{1}{\Gamma(\alpha)} \int_0^{t_{n+1}} B(\tau, S_{ph}, S_{cr}, X)(t_{n+1}-\tau)^{\alpha-1} d\tau. \tag{31}$$

$$X(t_{n+1}) - X(0) = \frac{1}{\Gamma(\alpha)} \int_0^{t_{n+1}} C(\tau, S_{ph}, S_{cr}, X)(t_{n+1}-\tau)^{\alpha-1} d\tau. \tag{32}$$

$$S_{ph}(t_{n+1}) - S_{ph}(0) = \frac{1}{\Gamma(\alpha)} \sum_{j=0}^{n} \int_{t_j}^{t_{j+1}} A(\tau, S_{ph}, S_{cr}, X)(t_{n+1}-\tau)^{\alpha-1} d\tau. \tag{33}$$

$$S_{cr}(t_{n+1}) - S_{cr}(0) = \frac{1}{\Gamma(\alpha)} \sum_{j=0}^{n} \int_{t_j}^{t_{j+1}} B(\tau, S_{ph}, S_{cr}, X)(t_{n+1}-\tau)^{\alpha-1} d\tau. \tag{34}$$

$$X(t_{n+1}) - X(0) = \frac{1}{\Gamma(\alpha)} \sum_{j=0}^{n} \int_{t_j}^{t_{j+1}} C(\tau, S_{ph}, S_{cr}, X)(t_{n+1}-\tau)^{\alpha-1} d\tau. \tag{35}$$

We use two-step Lagrange polynomial as:

$$p_j(\tau, S_{ph}, S_{cr}, X) = \frac{\tau - t_{j-1}}{t_j - t_{j-1}} A(t_j, S_{ph}, S_{cr}, X) - \frac{\tau - t_j}{t_j - t_{j-1}} A(t_{j-1}, S_{ph}, S_{cr}, X). \quad (36)$$

$$q_j(\tau, S_{ph}, S_{cr}, X) = \frac{\tau - t_{j-1}}{t_j - t_{j-1}} B(t_j, S_{ph}, S_{cr}, X) - \frac{\tau - t_j}{t_j - t_{j-1}} B(t_{j-1}, S_{ph}, S_{cr}, X). \quad (37)$$

$$s_j(\tau, S_{ph}, S_{cr}, X) = \frac{\tau - t_{j-1}}{t_j - t_{j-1}} C(t_j, S_{ph}, S_{cr}, X) - \frac{\tau - t_j}{t_j - t_{j-1}} C(t_{j-1}, S_{ph}, S_{cr}, X). \quad (38)$$

Then, we obtain

$$\begin{aligned} S_{ph}(t_{n+1}) - S_{ph}(0) &= \frac{1}{\Gamma(\alpha)} \sum_{j=0}^{n} \int_{t_j}^{t_{j+1}} p(\tau, S_{ph}, S_{cr}, X)(t_{n+1} - \tau)^{\alpha-1} d\tau \\ &= \sum_{j=0}^{n} \left[\frac{h^\alpha A(t_j, S_{ph}, S_{cr}, X)}{\Gamma(\alpha+2)} ((n+1-j)^\alpha (n-j+2+\alpha) \right. \\ &\quad \left. -(n-j)^\alpha (n-j+2+2\alpha))\right] \\ &\quad - \sum_{j=0}^{n} \left[\frac{h^\alpha A(t_{j-1}, S_{ph}, S_{cr}, X)}{\Gamma(\alpha+2)} \Big((n+1-j)^{\alpha+1} \right. \\ &\quad \left. -(n-j)^\alpha (n-j+1+\alpha))\right] \end{aligned}$$

$$\begin{aligned} S_{cr}(t_{n+1}) - S_{cr}(0) &= \frac{1}{\Gamma(\alpha)} \sum_{j=0}^{n} \int_{t_j}^{t_{j+1}} q(\tau, S_{ph}, S_{cr}, X)(t_{n+1} - \tau)^{\alpha-1} d\tau \\ &= \sum_{j=0}^{n} \left[\frac{h^\alpha B(t_j, S_{ph}, S_{cr}, X)}{\Gamma(\alpha+2)} ((n+1-j)^\alpha (n-j+2+\alpha) \right. \\ &\quad \left. -(n-j)^\alpha (n-j+2+2\alpha))\right] \\ &\quad - \sum_{j=0}^{n} \left[\frac{h^\alpha B(t_{j-1}, S_{ph}, S_{cr}, X)}{\Gamma(\alpha+2)} \Big((n+1-j)^{\alpha+1} \right. \\ &\quad \left. -(n-j)^\alpha (n-j+1+\alpha))\right] \end{aligned}$$

$$\begin{aligned} X(t_{n+1}) - X(0) &= \frac{1}{\Gamma(\alpha)} \sum_{j=0}^{n} \int_{t_j}^{t_{j+1}} s(\tau, S_{ph}, S_{cr}, X)(t_{n+1} - \tau)^{\alpha-1} d\tau \\ &= \sum_{j=0}^{n} \left[\frac{h^\alpha C(t_j, S_{ph}, S_{cr}, X)}{\Gamma(\alpha+2)} ((n+1-j)^\alpha (n-j+2+\alpha) \right. \\ &\quad \left. -(n-j)^\alpha (n-j+2+2\alpha))\right] \\ &\quad - \sum_{j=0}^{n} \left[\frac{h^\alpha C(t_{j-1}, S_{ph}, S_{cr}, X)}{\Gamma(\alpha+2)} \Big((n+1-j)^{\alpha+1} \right. \\ &\quad \left. -(n-j)^\alpha (n-j+1+\alpha))\right] \end{aligned}$$

Thus, the numerical scheme for the model with power law kernel has been obtained. We used this scheme and obtained Figures 1–4.

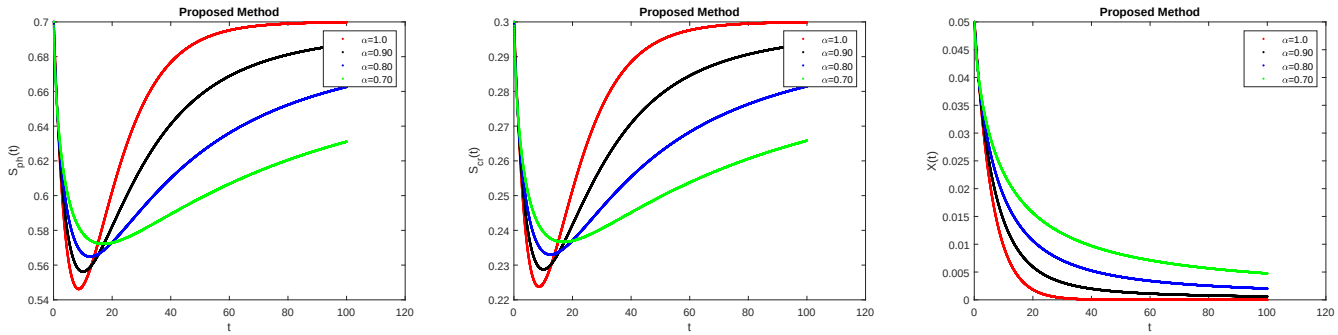

Figure 1. Solutions of (14)–(16) for $\beta = 1$, fractal dimension 1, and $\alpha = 1, 0.9, 0.8, 0.7$ with the power-law kernel.

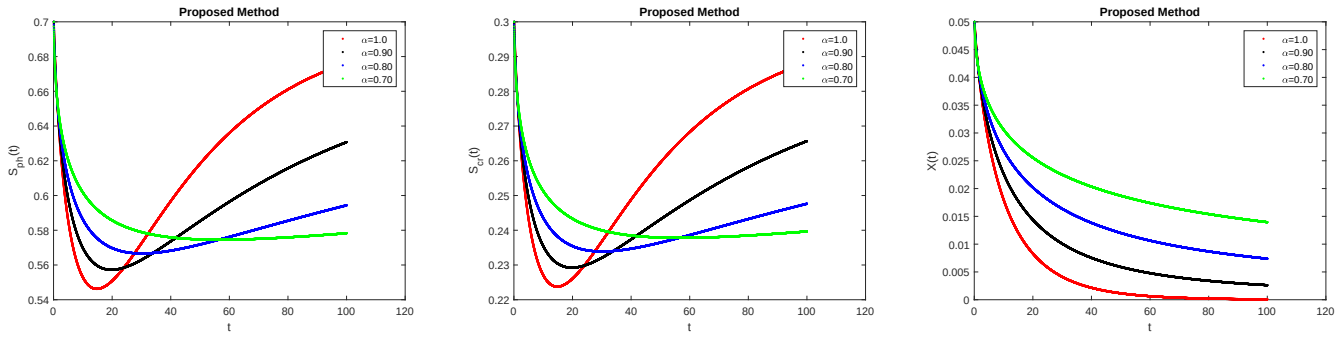

Figure 2. Solutions of (14)–(16) for $\beta = 1$, fractal dimension 0.8, and $\alpha = 1, 0.9, 0.8, 0.7$ with the power-law kernel.

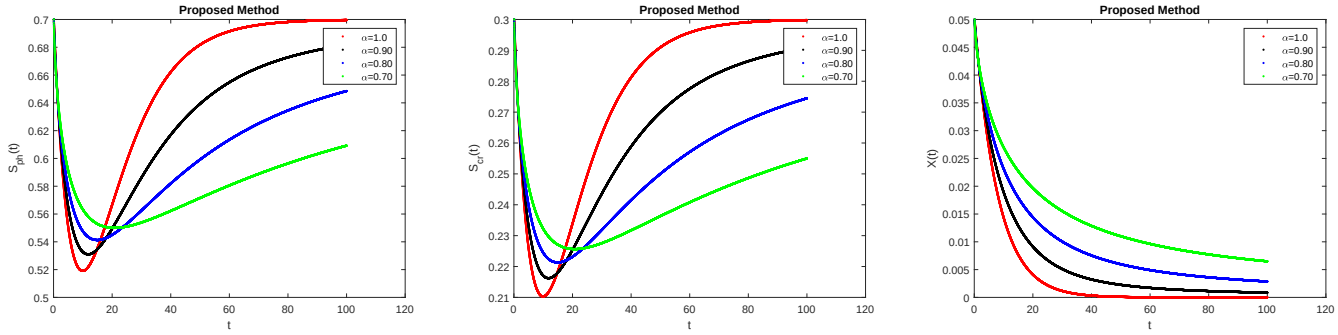

Figure 3. Solutions of (14)–(16) for $\beta = 0.5$, fractal dimension 1, and $\alpha = 1, 0.9, 0.8, 0.7$ with the power-law kernel.

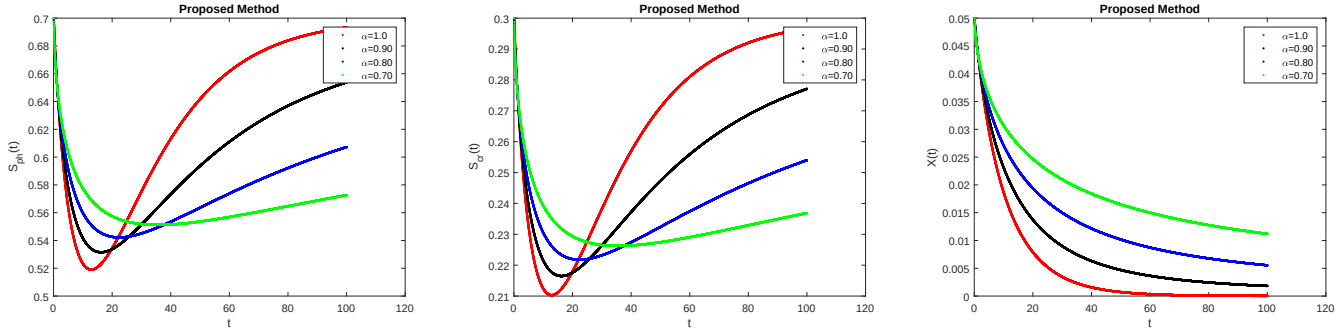

Figure 4. Solutions of (14)–(16) for $\beta = 0.5$, fractal dimension 0.9, and $\alpha = 1, 0.9, 0.8, 0.7$ with the power-law kernel.

5. Analysis of the Model with the Exponential-Decay Kernel

Next we analyze the model with using the exponential-decay kernel as:

$$ {}_0^{FFE}D_t^{\alpha,\eta} S_{ph} = D\Big(S_{ph0} - S_{ph}\Big) - k_{ph} \cdot \mu\Big(S_{ph}, S_{cr}\Big) \cdot X. \tag{39} $$

$$ {}_0^{FFE}D_t^{\alpha,\eta} S_{cr} = D(S_{cr0} - S_{cr}) - k_{cr} \cdot \mu\Big(S_{ph}, S_{cr}\Big) \cdot X. \tag{40} $$

$$ {}_0^{FFE}D_t^{\alpha,\eta} X = -D\beta X + \mu\Big(S_{ph}, S_{cr}\Big) X. \tag{41} $$

Using the relation between the classical derivative and the fractal derivative yields

$$ {}_0^{CF}D_t^{\alpha} S_{ph} = \eta t^{\eta-1}\Big(D\Big(S_{ph0} - S_{ph}\Big) - k_{ph} \cdot \mu\Big(S_{ph}, S_{cr}\Big) \cdot X\Big). \tag{42} $$

$$ {}_0^{CF}D_t^{\alpha} S_{cr} = \eta t^{\eta-1}\Big(D(S_{cr0} - S_{cr}) - k_{cr} \cdot \mu\Big(S_{ph}, S_{cr}\Big) \cdot X\Big). \tag{43} $$

$$ {}_0^{CF}D_t^{\alpha} X = \eta t^{\eta-1}\Big(-D\beta X + \mu\Big(S_{ph}, S_{cr}\Big) X\Big). \tag{44} $$

For simplicity, we define

$$ K(t, S_{ph}, S_{cr}, X) = \eta t^{\eta-1}\Big(D\Big(S_{ph0} - S_{ph}\Big) - k_{ph} \cdot \mu\Big(S_{ph}, S_{cr}\Big) \cdot X\Big). \tag{45} $$

$$ L(t, S_{ph}, S_{cr}, X) = \eta t^{\eta-1}\Big(D(S_{cr0} - S_{cr}) - k_{cr} \cdot \mu\Big(S_{ph}, S_{cr}\Big) \cdot X\Big). \tag{46} $$

$$ M(t, S_{ph}, S_{cr}, X) = \eta t^{\eta-1}\Big(-D\beta X + \mu\Big(S_{ph}, S_{cr}\Big) X\Big). \tag{47} $$

Then, we obtain

$$ {}_0^{CF}D_t^{\alpha} S_{ph} = K(t, S_{ph}, S_{cr}, X). \tag{48} $$

$$ {}_0^{CF}D_t^{\alpha} S_{cr} = L(t, S_{ph}, S_{cr}, X). \tag{49} $$

$$ {}_0^{CF}D_t^{\alpha} X = M(t, S_{ph}, S_{cr}, X). \tag{50} $$

Applying the CF integral yields [22]:

$$ \begin{aligned} S_{ph}(t) - S_{ph}(0) &= \frac{1-\alpha}{M(\alpha)} K(t, S_{ph}, S_{cr}, X) + \frac{\alpha}{M(\alpha)} \int_0^t K(\tau, S_{ph}, S_{cr}, X) d\tau. \\ S_{cr}(t) - S_{cr}(0) &= \frac{1-\alpha}{M(\alpha)} L(t, S_{ph}, S_{cr}, X) + \frac{\alpha}{M(\alpha)} \int_0^t L(\tau, S_{ph}, S_{cr}, X) d\tau. \\ X(t) - X(0) &= \frac{1-\alpha}{M(\alpha)} M(t, S_{ph}, S_{cr}, X) + \frac{\alpha}{M(\alpha)} \int_0^t M(\tau, S_{ph}, S_{cr}, X) d\tau. \end{aligned} $$

Discretizing the above equations at t_{n+1} and t_n, we receive:

$$ \begin{aligned} S_{ph}^{n+1} &= S_{ph}^0 + \frac{1-\alpha}{M(\alpha)} K(t_n, S_{ph}^n, S_{cr}^n, X^n) \\ &\quad + \frac{\alpha}{M(\alpha)} \int_0^{t_{n+1}} K(\tau, S_{ph}, S_{cr}, X) d\tau \\ S_{cr}^{n+1} &= S_{cr}^0 + \frac{1-\alpha}{M(\alpha)} L(t_n, S_{ph}^n, S_{cr}^n, X^n) \\ &\quad + \frac{\alpha}{M(\alpha)} \int_0^{t_{n+1}} L(\tau, S_{ph}, S_{cr}, X) d\tau \\ X^{n+1} &= X^0 + \frac{1-\alpha}{M(\alpha)} M(t_n, S_{ph}^n, S_{cr}^n, X^n) \\ &\quad + \frac{\alpha}{M(\alpha)} \int_0^{t_{n+1}} M(\tau, S_{ph}, S_{cr}, X) d\tau \end{aligned} $$

and

$$\begin{aligned}
S_{ph}^{n} &= S_{ph}^{0}+\frac{1-\alpha}{M(\alpha)}K(t_{n-1},S_{ph}^{n-1},S_{cr}^{n-1},X^{n-1})\\
&\quad+\frac{\alpha}{M(\alpha)}\int_{0}^{t_n}K(\tau,S_{ph},S_{cr},X)d\tau\\
S_{cr}^{n} &= S_{cr}^{0}+\frac{1-\alpha}{M(\alpha)}L(t_{n-1},S_{ph}^{n-1},S_{cr}^{n-1},X^{n-1})\\
&\quad+\frac{\alpha}{M(\alpha)}\int_{0}^{t_n}L(\tau,S_{ph},S_{cr},X)d\tau\\
X^{n} &= X^{0}+\frac{1-\alpha}{M(\alpha)}M(t_{n-1},S_{ph}^{n-1},S_{cr}^{n-1},X^{n-1})\\
&\quad+\frac{\alpha}{M(\alpha)}\int_{0}^{t_n}M(\tau,S_{ph},S_{cr},X)d\tau
\end{aligned}$$

Thus, we reach

$$\begin{aligned}
S_{ph}^{n+1} &= S_{ph}^{n}+\frac{1-\alpha}{M(\alpha)}\Big(K(t_n,S_{ph}^{n},S_{cr}^{n},X^{n})-K(t_{n-1},S_{ph}^{n-1},S_{cr}^{n-1},X^{n-1})\Big)\\
&\quad+\frac{\alpha}{M(\alpha)}\int_{t_n}^{t_{n+1}}K(\tau,S_{ph},S_{cr},X)d\tau\\
S_{cr}^{n+1} &= S_{cr}^{n}+\frac{1-\alpha}{M(\alpha)}\Big(L(t_n,S_{ph}^{n},S_{cr}^{n},X^{n})-L(t_{n-1},S_{ph}^{n-1},S_{cr}^{n-1},X^{n-1})\Big)\\
&\quad+\frac{\alpha}{M(\alpha)}\int_{t_n}^{t_{n+1}}L(\tau,S_{ph},S_{cr},X)d\tau\\
X^{n+1} &= X^{n}+\frac{1-\alpha}{M(\alpha)}\Big(M(t_n,S_{ph}^{n},S_{cr}^{n},X^{n})-M(t_{n-1},S_{ph}^{n-1},S_{cr}^{n-1},X^{n-1})\Big)\\
&\quad+\frac{\alpha}{M(\alpha)}\int_{t_n}^{t_{n+1}}M(\tau,S_{ph},S_{cr},X)d\tau
\end{aligned}$$

Using the two-step Lagrange polynomial yields, we receive:

$$\begin{aligned}
S_{ph}^{n+1} &= S_{ph}^{n}+\frac{1-\alpha}{M(\alpha)}\Big(K(t_n,S_{ph}^{n},S_{cr}^{n},X^{n})-K(t_{n-1},S_{ph}^{n-1},S_{cr}^{n-1},X^{n-1})\Big)\\
&\quad+\frac{\alpha}{M(\alpha)}\left(\frac{3h}{2}K(t_n,S_{ph}^{n},S_{cr}^{n},X^{n})-\frac{h}{2}K(t_{n-1},S_{ph}^{n-1},S_{cr}^{n-1},X^{n-1})\right)\\
S_{cr}^{n+1} &= S_{cr}^{n}+\frac{1-\alpha}{M(\alpha)}\Big(L(t_n,S_{ph}^{n},S_{cr}^{n},X^{n})-L(t_{n-1},S_{ph}^{n-1},S_{cr}^{n-1},X^{n-1})\Big)\\
&\quad+\frac{\alpha}{M(\alpha)}\left(\frac{3h}{2}L(t_n,S_{ph}^{n},S_{cr}^{n},X^{n})-\frac{h}{2}L(t_{n-1},S_{ph}^{n-1},S_{cr}^{n-1},X^{n-1})\right)\\
X^{n+1} &= X^{n}+\frac{1-\alpha}{M(\alpha)}\Big(M(t_n,S_{ph}^{n},S_{cr}^{n},X^{n})-M(t_{n-1},S_{ph}^{n-1},S_{cr}^{n-1},X^{n-1})\Big)\\
&\quad+\frac{\alpha}{M(\alpha)}\left(\frac{3h}{2}M(t_n,S_{ph}^{n},S_{cr}^{n},X^{n})-\frac{h}{2}M(t_{n-1},S_{ph}^{n-1},S_{cr}^{n-1},X^{n-1})\right)
\end{aligned}$$

Thus, the numerical scheme for the model with exponential decay kernel has been obtained. We used this scheme and obtained Figures 5–8.

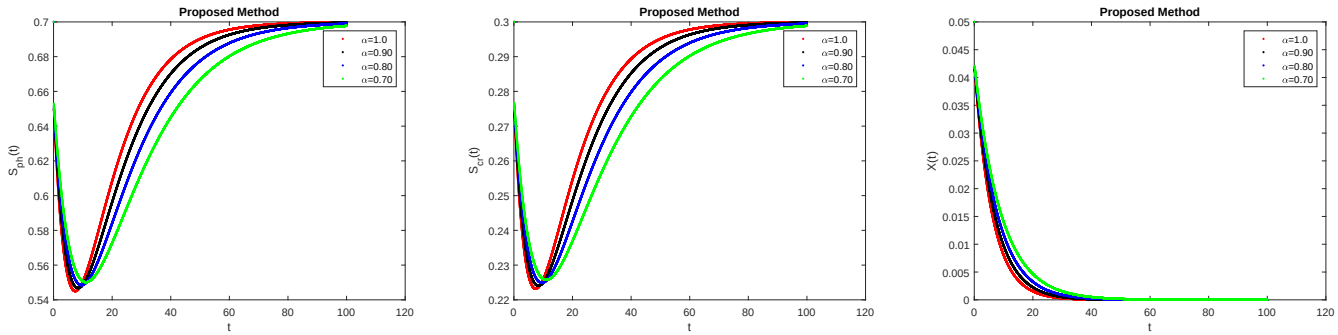

Figure 5. Solutions of (39)–(41) for $\beta = 1$, fractal dimension 1, and $\alpha = 1, 0.9, 0.8$, and 0.7 with exponential decay kernel.

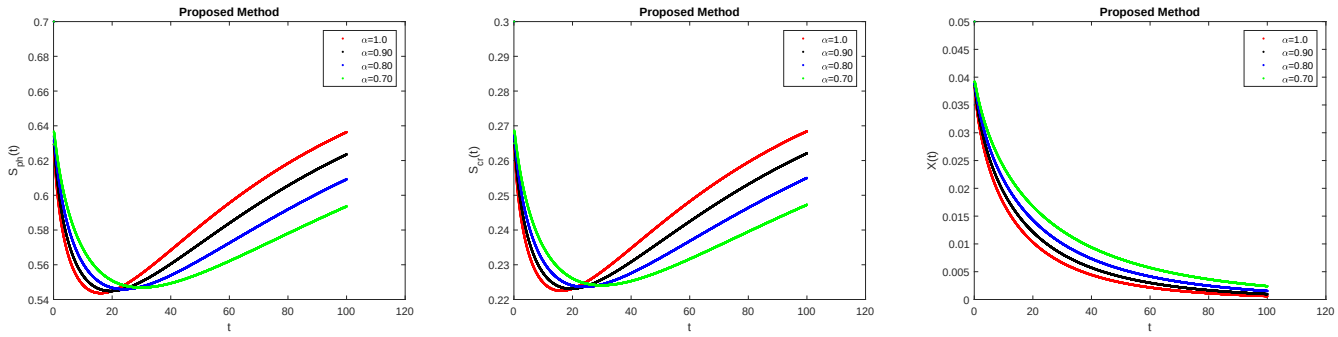

Figure 6. Solutions of (39)–(41) for $\beta = 1$, fractal dimension 0.7, and $\alpha = 1, 0.9, 0.8$, and 0.7 with exponential decay kernel.

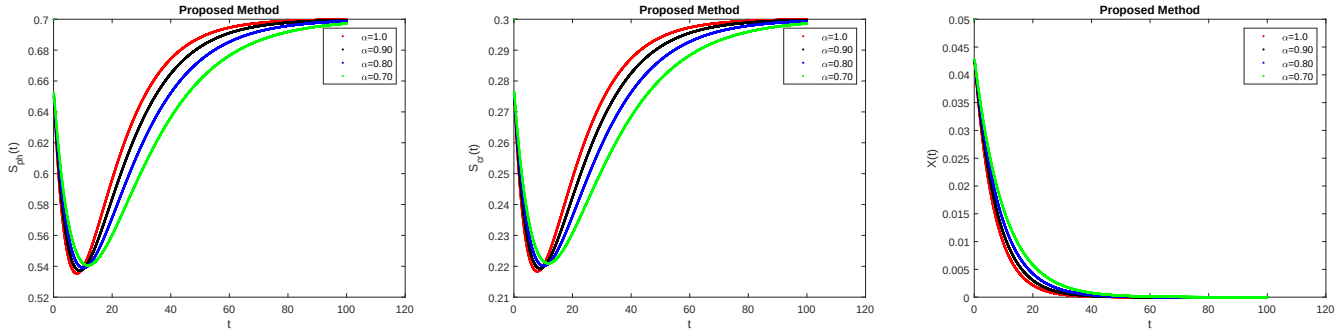

Figure 7. Solutions of (39)–(41) for $\beta = 0.8$, fractal dimension 1, and $\alpha = 1, 0.9, 0.8$, and 0.7 with exponential decay kernel.

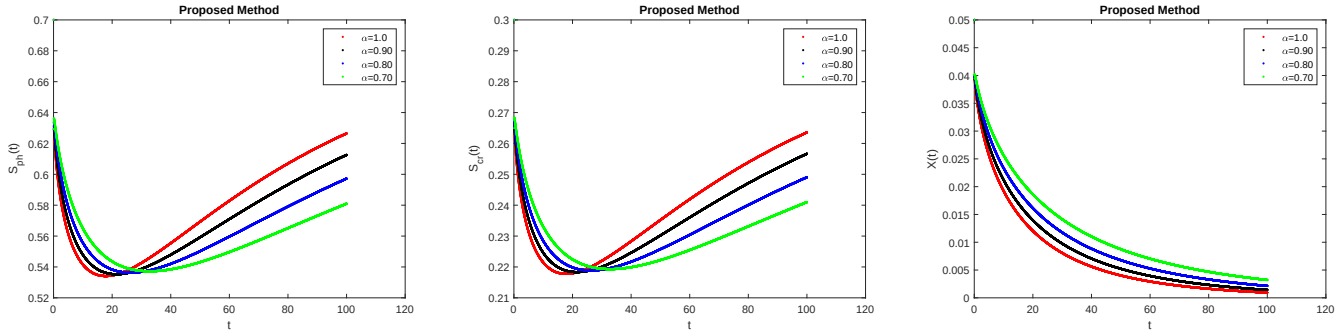

Figure 8. Solutions of (39)–(41) for $\beta = 0.8$, fractal dimension 0.7, and $\alpha = 1, 0.9, 0.8$, and 0.7 with exponential decay kernel.

6. Analysis of the Model with the Mittag–Leffler Kernel

Now, we analyze the model with fractional differentiation operator using the Mittag–Leffler kernel as:

$$ {}_0^{FFM}D_t^{\alpha,\eta} S_{ph} = D\Big(S_{ph0} - S_{ph}\Big) - k_{ph} \cdot \mu\Big(S_{ph}, S_{cr}\Big) \cdot X. \tag{51} $$

$$ {}_0^{FFM}D_t^{\alpha,\eta} S_{cr} = D(S_{cr0} - S_{cr}) - k_{cr} \cdot \mu\Big(S_{ph}, S_{cr}\Big) \cdot X. \tag{52} $$

$$ {}_0^{FFM}D_t^{\alpha,\eta} X = -D\beta X + \mu\Big(S_{ph}, S_{cr}\Big) X. \tag{53} $$

Then, we obtain

$$ {}_0^{AB}D_t^{\alpha} S_{ph} = \eta t^{\eta-1}\Big(D\Big(S_{ph0} - S_{ph}\Big) - k_{ph} \cdot \mu\Big(S_{ph}, S_{cr}\Big) \cdot X\Big). \tag{54} $$

$$ {}_0^{AB}D_t^{\alpha} S_{cr} = \eta t^{\eta-1}\Big(D(S_{cr0} - S_{cr}) - k_{cr} \cdot \mu\Big(S_{ph}, S_{cr}\Big) \cdot X\Big). \tag{55} $$

$$ {}_0^{AB}D_t^{\alpha} X = \eta t^{\eta-1}\Big(-D\beta X + \mu\Big(S_{ph}, S_{cr}\Big) X\Big). \tag{56} $$

For simplicity, we define

$$ Y(t, S_{ph}, S_{cr}, X) = \eta t^{\eta-1}\Big(D\Big(S_{ph0} - S_{ph}\Big) - k_{ph} \cdot \mu\Big(S_{ph}, S_{cr}\Big) \cdot X\Big). \tag{57} $$

$$ Z(t, S_{ph}, S_{cr}, X) = \eta t^{\eta-1}\Big(D(S_{cr0} - S_{cr}) - k_{cr} \cdot \mu\Big(S_{ph}, S_{cr}\Big) \cdot X\Big). \tag{58} $$

$$ T(t, S_{ph}, S_{cr}, X) = \eta t^{\eta-1}\Big(-D\beta X + \mu\Big(S_{ph}, S_{cr}\Big) X\Big). \tag{59} $$

Then, we receive

$$ {}_0^{AB}D_t^{\alpha} S_{ph} = Y(t, S_{ph}, S_{cr}, X). \tag{60} $$

$$ {}_0^{AB}D_t^{\alpha} S_{cr} = Z(t, S_{ph}, S_{cr}, X). \tag{61} $$

$$ {}_0^{AB}D_t^{\alpha} X = T(t, S_{ph}, S_{cr}, X). \tag{62} $$

Applying the AB integral gives:

$$ \begin{aligned} S_{ph}(t) - S_{ph}(0) &= \frac{1-\alpha}{AB(\alpha)} Y(t, S_{ph}, S_{cr}, X) + \frac{\alpha}{AB(\alpha)\Gamma(\alpha)} \int_0^t (t-p)^{\alpha-1} Y(p, S_{ph}, S_{cr}, X) dp. \\ S_{cr}(t) - S_{cr}(0) &= \frac{1-\alpha}{AB(\alpha)} Z(t, S_{ph}, S_{cr}, X) + \frac{\alpha}{AB(\alpha)\Gamma(\alpha)} \int_0^t (t-p)^{\alpha-1} Z(p, S_{ph}, S_{cr}, X) dp. \\ X(t) - X(0) &= \frac{1-\alpha}{AB(\alpha)} T(t, S_{ph}, S_{cr}, X) + \frac{\alpha}{AB(\alpha)\Gamma(\alpha)} \int_0^t (t-p)^{\alpha-1} T(p, S_{ph}, S_{cr}, X) dp. \end{aligned} $$

Discretizing the above equations at t_{n+1}, we receive:

$$
\begin{aligned}
S_{ph}^{n+1} &= S_{ph}^{0} + \frac{1-\alpha}{AB(\alpha)} Y(t_{n+1}, S_{ph}^{n}, S_{cr}^{n}, X^{n}) \\
&\quad + \frac{\alpha}{AB(\alpha)\Gamma(\alpha)} \int_{0}^{t_{n+1}} (t_{n+1}-p)^{\alpha-1} Y(p, S_{ph}, S_{cr}, X) dp \\
S_{cr}^{n+1} &= S_{cr}^{0} + \frac{1-\alpha}{AB(\alpha)} Z(t_{n+1}, S_{ph}^{n}, S_{cr}^{n}, X^{n}) \\
&\quad + \frac{\alpha}{AB(\alpha)\Gamma(\alpha)} \int_{0}^{t_{n+1}} (t_{n+1}-p)^{\alpha-1} Z(p, S_{ph}, S_{cr}, X) dp \\
X^{n+1} &= X^{0} + \frac{1-\alpha}{AB(\alpha)} T(t_{n+1}, S_{ph}^{n}, S_{cr}^{n}, X^{n}) \\
&\quad + \frac{\alpha}{AB(\alpha)\Gamma(\alpha)} \int_{0}^{t_{n+1}} (t_{n+1}-p)^{\alpha-1} T(p, S_{ph}, S_{cr}, X) dp
\end{aligned}
$$

Then, we obtain

$$
\begin{aligned}
S_{ph}^{n+1} &= S_{ph}^{0} + \frac{1-\alpha}{AB(\alpha)} Y(t_{n+1}, S_{ph}^{n}, S_{cr}^{n}, X^{n}) \\
&+ \frac{\alpha}{AB(\alpha)} \sum_{i=0}^{n} \left[\frac{h^{\alpha} Y(t_i, S_{ph}^{n}, S_{cr}^{n}, X^{n})}{\Gamma(\alpha+2)} ((n+1-i)^{\alpha}(n-i+2+\alpha) \right. \\
&\left. -(n-i)^{\alpha}(n-i+2+2\alpha)) \right] \\
&- \frac{\alpha}{AB(\alpha)} \sum_{i=0}^{n} \left[\frac{h^{\alpha} Y(t_{i-1}, S_{ph}^{n-1}, S_{cr}^{n-1}, X^{n-1})}{\Gamma(\alpha+2)} \Big((n+1-i)^{\alpha+1} \right. \\
&\left. -(n-i)^{\alpha}(n-i+1+\alpha)) \right]
\end{aligned}
$$

$$
\begin{aligned}
S_{cr}^{n+1} &= S_{cr}^{0} + \frac{1-\alpha}{AB(\alpha)} Z(t_{n+1}, S_{ph}^{n}, S_{cr}^{n}, X^{n}) \\
&+ \frac{\alpha}{AB(\alpha)} \sum_{i=0}^{n} \left[\frac{h^{\alpha} Z(t_i, S_{ph}^{n}, S_{cr}^{n}, X^{n})}{\Gamma(\alpha+2)} ((n+1-i)^{\alpha}(n-i+2+\alpha) \right. \\
&\left. -(n-i)^{\alpha}(n-i+2+2\alpha)) \right] \\
&- \frac{\alpha}{AB(\alpha)} \sum_{i=0}^{n} \left[\frac{h^{\alpha} Z(t_{i-1}, S_{ph}^{n-1}, S_{cr}^{n-1}, X^{n-1})}{\Gamma(\alpha+2)} \Big((n+1-i)^{\alpha+1} \right. \\
&\left. -(n-i)^{\alpha}(n-i+1+\alpha)) \right]
\end{aligned}
$$

$$
\begin{aligned}
X^{n+1} &= X^{0} + \frac{1-\alpha}{AB(\alpha)} T(t_{n+1}, S_{ph}^{n}, S_{cr}^{n}, X^{n}) \\
&+ \frac{\alpha}{AB(\alpha)} \sum_{i=0}^{n} \left[\frac{h^{\alpha} T(t_i, S_{ph}^{n}, S_{cr}^{n}, X^{n})}{\Gamma(\alpha+2)} ((n+1-i)^{\alpha}(n-i+2+\alpha) \right. \\
&\left. -(n-i)^{\alpha}(n-i+2+2\alpha)) \right] \\
&- \frac{\alpha}{AB(\alpha)} \sum_{i=0}^{n} \left[\frac{h^{\alpha} T(t_{i-1}, S_{ph}^{n-1}, S_{cr}^{n-1}, X^{n-1})}{\Gamma(\alpha+2)} \Big((n+1-i)^{\alpha+1} \right. \\
&\left. -(n-i)^{\alpha}(n-i+1+\alpha)) \right].
\end{aligned}
$$

Thus, the numerical scheme for the model with Mittag–Leffler kernel has been obtained. We used this scheme and obtained Figures 9–12.

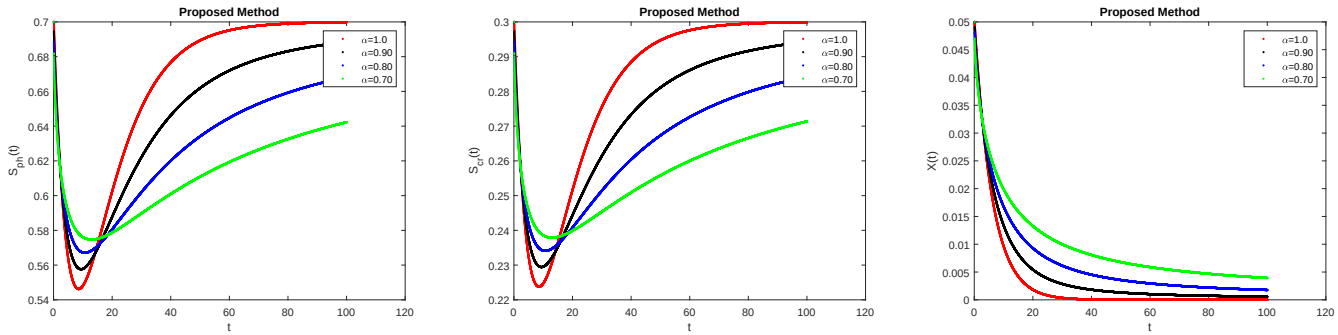

Figure 9. Solutions of (54)–(56) for $\beta = 1$, fractal dimension 1, and $\alpha = 1, 0.9, 0.8$, and 0.7 with Mittag–Leffler kernel.

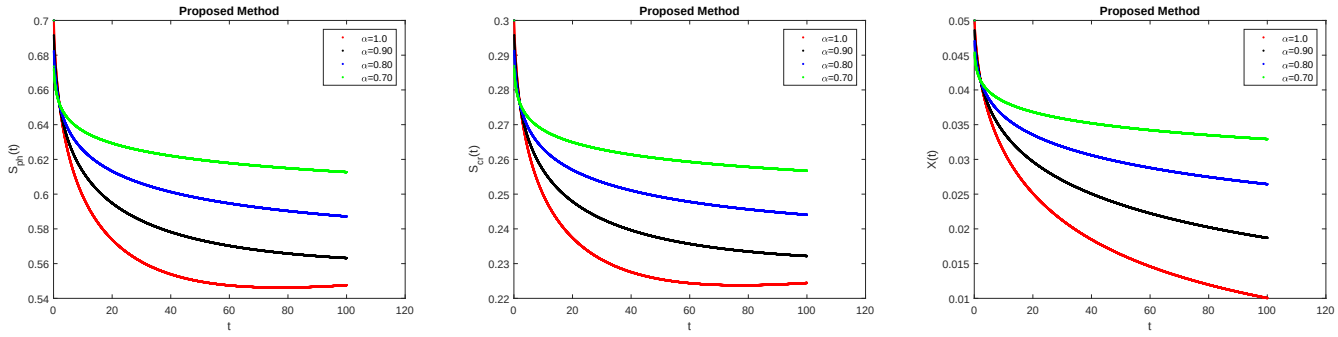

Figure 10. Solutions of (39)–(41) for $\beta = 1$, fractal dimension 0.5, and $\alpha = 1, 0.9, 0.8$, and 0.7 with Mittag–Leffler kernel.

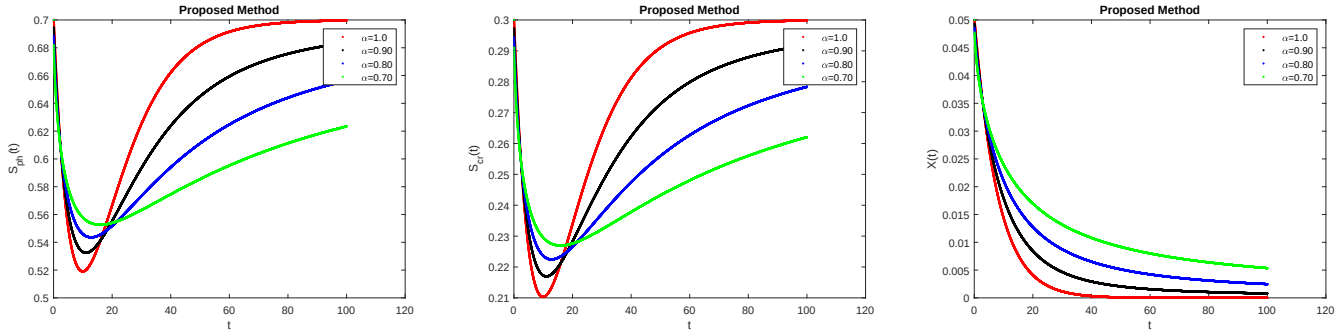

Figure 11. Solutions of (39)–(41) for $\beta = 0.5$, fractal dimension 1, and $\alpha = 1, 0.9, 0.8$, and 0.7 with Mittag–Leffler kernel.

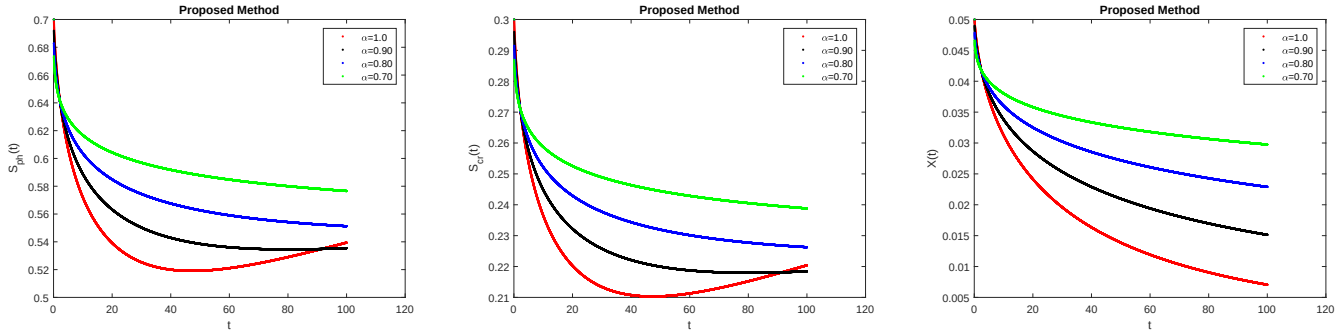

Figure 12. Solutions of (39)–(41) for $\beta = 0.5$, fractal dimension 0.6, and $\alpha = 1, 0.9, 0.8$, and 0.7 with Mittag–Leffler kernel.

Remark 1. *A valuable and huge benefit of fractional differentiation operator is that we can formulate models better defining the systems with memory effects. It is known that the use of integro-*

differential kernels of a certain type in integro-differential equations leads us to the fractional derivative operator [31]. The kernels with degree functions in integro-differential equations of the Voltaire type [32], allow us to describe this memory effect [33,34].

Fractal–fractional operators with different memories are related to the non-local dynamical systems' different types of relaxation processes. Thus, models with fractional differentiation operators are more effective and valuable.

7. Results and Discussions

In this section, we present numerical simulations for different fractional order and fractal dimension values. We also add the classical derivative with the integer fractal dimension equal to 1.

We chose fractal dimension as the integer and noninteger in the figures. We discuss the results with the three kernels described in Sections 5–7. The figures α, β, and η are between zero and one. In these simulations, β is the parameter given on the model, η is the fractal dimension, and α is the fractional order. We see the effect of the fractional order α under different kernels and values of the parameter β and the fractal dimension η. Figures 1 and 2 show the numerical simulations for $\beta = 1$, the fractal dimensions $\eta = 1$ and $\eta = 0.8$, and for different fractional order α values with the power-law kernel. We also show how this kernel behaves for $\beta = 0.5$ and the fractal dimension $\eta = 1$ and $\eta = 0.9$ in Figures 3 and 4. We see that the convergence is faster for the case $\beta = 1$ than to the case $\beta = 0.5$, as long as the fractal dimension is close to 1. The concentrations $S_{ph}(t)$ and $S_{cr}(t)$ decrease as long as α decreases. In all the cases, the concentration $X(t)$ decreases to 0.

The results for the exponential-decay kernel are shown for $\beta = 1$ in Figure 5 (with fractal dimension $\eta = 1$) and Figure 6 (with fractal dimension $\eta = 0.7$). We demonstrate the results for $\beta = 0.8$ and $\eta = 1$ (Figure 7) and $\eta = 0.7$ (Figure 8). Despite varying the parameters β, α, and the fractal dimension, there are fewer differences in the concentrations with respect to the results shown by the power-law kernel.

Finally, in Figures 9–12, we show the results for the Mittag–Leffler kernel. The numerical simulations for $\beta = 1$ are shown in Figure 9 ($\eta = 1$) and Figure 10 ($\eta = 0.5$). We also see the behavior of the solution for $\beta = 0.5, \eta = 1$ in Figure 11 and $\beta = 0.5, \eta = 0.6$ in Figure 12.

We have seen that the exponential-decay kernel is the one that converges faster to the equilibrium, with the smaller difference among concentrations of the substances.

8. Conclusions

This work provides a mathematical model for breaking down a phenol and p-cresol mixture in a bioreactor with continuous stirring. Three nonlinear ordinary differential equations served as the foundation for the model. The equilibrium points of the model were identified, and their stability was examined and shown. Additionally, we used the fractional differentiation operator to examine the model and three distinct kernels to examine the effects of the fractal dimension and fractional order. We developed very efficient numerical algorithms for biomass, phenol, and p-cresol concentrations. To demonstrate the accuracy of the suggested approach, we offered numerical simulations for different α and β values. The right choice of model parameters would require validation with experimental data.

Author Contributions: Conceptualization, A.A. and J.A.C.; methodology, A.A. and J.A.C.; software, A.A.; formal analysis, A.A. and J.A.C.; investigation, A.A. and J.A.C.; writing—original draft preparation, A.A.; writing—review and editing, A.A. and J.A.C. All authors have read and agreed to the published version of the manuscript.

Funding: JAC is supported by Generalitat Valenciana, Project PROMETEO CIPROM/2022/21.

Data Availability Statement: All data used in this work has been obtained from the mathematical formulas described in the paper.

Conflicts of Interest: The authors declare no conflicts of interest.

References

1. Dimitrova, N.; Zlateva, P. Global stability analysis of a bioreactor model for phenol and cresol mixture degradation. *Processes* **2021**, *9*, 124. [CrossRef]
2. Seo, J.S.; Keum, Y.S.; Li, Q.X. Bacterial degradation of aromatic compounds. *Int. J. Environ. Res. Public Health* **2009**, *6*, 278–309. [CrossRef]
3. Sharma, N.K.; Philip, L.; Bhallamudi, S.M. Aerobic degradation of phenolics and aromatic hydrocarbons in presence of cyanide. *Bioresour. Technol.* **2012**, *121*, 263–273. [CrossRef]
4. Tomei, M.C.; Annesini, M.C. Biodegradation of phenolic mixtures in a sequencing batch reactor: A kinetic study. *Environ. Sci. Pollut. Res.* **2008**, *15*, 188–195. [CrossRef]
5. Yemendzhiev, H.; Zlateva, P.; Alexieva, Z. Comparison of the biodegradation capacity of two fungal strains toward a mixture of phenol and cresol by mathematical modeling. *Biotechnol. Biotechnol. Equip.* **2012**, *26*, 3278–3281. [CrossRef]
6. Kietkwanboot, A.; Chaiprapat, S.; Müller, R.; Suttinun, O. Biodegradation of phenolic compounds present in palm oil mill effluent as single and mixed substrates by Trameteshirsuta AK04. *J. Environ. Sci. Health Part A Toxic/Hazard. Subst. Environ. Eng.* **2020**, *55*, 989–1002.
7. Momani, S. An explicit and numerical solutions of the fractional KdV equation. *Math. Comput. Simul.* **2005**, *70*, 110–118. [CrossRef]
8. Li, C.; Cao, J. A finite difference method for time-fractional telegraph equation. In Proceedings of the IEEE/ASME International Conference on Mechatronics and Embedded Systems and Applications (MESA), Suzhou, China, 8–10 July 2012; pp. 314–318.
9. Huang, F.; Liu, F. The fundamental solution of the space-time fractional advection-dispersion equation. *J. Appl. Math. Comput.* **2005**, *18*, 21–36. [CrossRef]
10. Bhrawy, A.H.; Doha, E.H.; Ezz-Eldien, S.S.; Van Gorder, R.A. A new Jacobi spectral collocation method for solving $(1+1)$fractional Schrodinger equations and fractional coupled Schrodinger systems. *Eur. Phys. J. Plus.* **2014**, *129*, 260. [CrossRef]
11. Karatay, T.; Bayramoglu, S.R.; Sahin, A. Implicit difference approximation for the time fractional heat equation with the nonlocal condition. *Appl. Numer. Math.* **2011**, *61*, 1281–1288. [CrossRef]
12. Chen, Y.; Yi, M.; Chen, C.; Yu, C. Bernstein polynomials method for fractional convection-diffusion equation with variable coefficients. *Comput. Model. Eng. Sci.* **2012**, *83*, 639–653.
13. Liu, F.; Anh, V.; Turner, I. Numerical solution of space fractional FokkerPlanck equation. *J. Comp. Appl. Math.* **2004**, *166*, 209–219. [CrossRef]
14. Fuente, D.; Lizama, C.; Urchueguía, J.F.; Conejero, J.A. Estimation of the light field inside photosynthetic microorganism cultures through Mittag-Leffler functions at depleted light conditions. *J. Quant. Spectrosc. Radiat. Transf.* **2018**, *204*, 23–26. [CrossRef]
15. Lizama, C.; Murillo-Arcila, M.; Trujillo, M. Fractional Beer-Lambert law in laser heating of biological tissue. *AIMS Math.* **2022**, *14*, 14444–14459. [CrossRef]
16. Momani, S.; Odibat, Z. Comparison between the homotopy perturbation method and the variational iteration method for linear fractional partial differential equations. *Comput. Math. Appl.* **2007**, *54*, 910–919. [CrossRef]
17. El-Sayed, A.M.A.; Gaber, M. The Adomian decomposition method for solving partial differential equations of fractal order in finite domains. *Phys. Lett. A* **2006**, *359*, 175–182. [CrossRef]
18. Ahmad, H.; Khan, M.N.; Ahmad, I.; Omri, M.; Alotaibi, M.F. A meshless method for numerical solutions of linear and nonlinear time-fractional Black-Scholes models. *AIMS Math.* **2023**, *8*, 19677–19698. [CrossRef]
19. Khaliq, S.; Ahmad, S.; Ullah, A.; Ahmad, H.; Saifullah, S.; Nofal, T.A. New waves solutions of the (2 + 1)-dimensional generalized Hirota–Satsuma–Ito equation using a novel expansion method. *Res. Phys.* **2023**, *50*, 106450. [CrossRef]
20. Adel, M.; Khader, M.M.; Ahmad, H.; Assiri, T.A. Approximate analytical solutions for the blood ethanol concentration system and predator-prey equations by using variational iteration method. *AIMS Math.* **2023**, *8*, 19083–19096. [CrossRef]
21. Atangana, A. Fractal-fractional differentiation and integration: Connecting fractal calculus and fractional calculus to predict complex, system. *Chaos Solitons Fractals* **2017**, *102*, 396–406. [CrossRef]
22. Toufik, M.; Atangana, A. New numerical approximation of fractional derivative with non-local and non-singular kernel: Application to chaotic models. *Eur. Phys. J. Plus* 132, **2017**, *10*, 444. [CrossRef]
23. Mohammadi, H.; Kumar, S.; Rezapour, S.; Etemad, S. A theoretical study of the Caputo-Fabrizio fractional modeling for hearing loss due to Mumps virus with optimal control. *Chaos Solitons Fractals* **2021**, *144*, 110668. [CrossRef]
24. Baleanu, D.; Jajarmi, A.; Mohammadi, H.; Rezapour, S. A new study on the mathematical modelling of human liver with Caputo-Fabrizio fractional derivative. *Chaos Solitons Fractals* **2021**, *134*, 109705. [CrossRef]
25. Alzabut, J.; Selvam, A.; Dhineshbabu, R.; Tyagi, S.; Ghaderi, M.; Rezapour, S. A Caputo discrete fractional-order thermostat model with one and two sensors fractional boundary conditions depending on positive parameters by using the Lipschitz-type inequality. *J. Inequal. Appl.* **2022**, *2022*, 56. [CrossRef]
26. Heydarpour, Z.; Izadi, J.; George, R.; Ghaderi, M.; Rezapour, S. On a partial fractional hybrid version of generalized Sturm–Liouville–Langevin equation. *Fractal Fract.* **2022**, *6*, 269. [CrossRef]
27. George, R.; Houas, M.; Ghaderi, M.; Rezapour, S.; Elagan, S.K. On a coupled system of pantograph problem with three sequential fractional derivatives by using positive contraction-type inequalities. *Results Phys.* **2022**, *39*, 105687. [CrossRef]
28. Matar, M.M.; Abbas, M.I.; Alzabut, J.; Kaabar, M.K.A.; Etemad, S.; Rezapour, S. Investigation of the p-Laplacian nonperiodic nonlinear boundary value problem via generalized Caputo fractional derivatives. *Adv. Differ. Equ.* **2021**, *2021*, 68. [CrossRef]

29. Etemad, S.; Avci, I.; Kumar, P.; Baleanu, D.; Rezapour, S. Some novel mathematical analysis on the fractal-fractional model of the AH1N1/09 virus and its generalized Caputo-type version. *Chaos Solitons Fractals* **2022**, *162*, 112511. [CrossRef]
30. Ullah, I.; Ullah, A.; Ahmad, S.; Ahmad, H.; Nofal, T.A. A survey of KdV-CDG equations via nonsingular fractional operators. *AIMS Math.* **2023**, *8*, 18964–18981. [CrossRef]
31. Kilbas, A.A.; Srivastava, H.M.; Trujillo, J.J. *Theory and Applications of Fractional Differential Equations*; Elsevier: Amsterdam, The Netherlands, 2006; Volume 204, 523p.
32. Volterra, V. Sur les équations intégro-différentielles et leurs applications. *Acta Math.* **1912**, *35*, 295–356. [CrossRef]
33. Coimbra, C.F. Mechanics with variable-order differential operators. *Ann. Phys.* **2003**, *12*, 11–12. [CrossRef]
34. Ortigueira, M.D.; Valerio, D.; Machado, J.T. Variable order fractional systems. *Commun. Nonlinear Sci. Numer. Simul.* **2019**, *71*, 231–243. [CrossRef]